

ON THE PREDOMINANCE OF THE RADIAL COMPONENT OF THE MAGNETIC FIELD IN THE SOLAR CORONA

SHADIA RIFAI HABBAL

University of Wales, Aberystwyth, Ceredigion SY23 3BZ, UK; and Harvard-Smithsonian Center for Astrophysics, 60 Garden Street, Cambridge, MA 02138

RICHARD WOO

Jet Propulsion Laboratory, California Institute of Technology, 4800 Oak Grove Drive, Pasadena, CA 91109

AND

JEAN ARNAUD

Laboratoire d'Astrophysique, Université Paul Sabatier, Toulouse, France

Received 2001 February 21; accepted 2001 May 14

ABSTRACT

Polarimetric measurements of the corona out to $2 R_{\odot}$ in the Fe XIII 10747 Å line, the strongest of the iron forbidden lines, are placed for the first time in the context of spatially resolved images of coronal density structures. These measurements, which are the only tool currently available to yield the direction of the magnetic field, date to 1980, the only year when they were available with polarized brightness images of the corona. Through this comparison, the observed predominance of the radial component of the coronal magnetic field, discovered over three decades ago from eclipse observations and established systematically by Arnaud, is shown to point to the coexistence of two magnetic field components in the corona: a nonradial field associated with the large-scale structures known as streamers and a more pervasive radial magnetic field. This finding suggests that these two components are the coronal counterparts of the strong- and weak-field components recently observed in the quiet-Sun photospheric field and supported by recent theoretical investigations of the solar dynamo.

Subject heading: polarization — solar wind — Sun: corona — Sun: infrared — Sun: magnetic fields

1. INTRODUCTION

Following decades of ground- and space-based observations of the Sun, it has become clear that the magnetic field controls the distribution of coronal density structures. Surprisingly, however, no straightforward technique exists at present for the measurement of the coronal magnetic field. Our impression of its direction has been largely influenced by white light images and coronal emission observed during eclipses or with coronagraphs and by space observations in the extreme ultraviolet and X-ray wavelengths. Attempts at quantifying this impression have been made with different mathematical methods and approximations, using the observed line of sight component of the photospheric field as a starting point (e.g., Altschuler & Newkirk 1969; Linker et al. 1999).

The structure of the coronal magnetic field thus developed has subsequently influenced our view on the origin of the fast solar wind. Measured first in the ecliptic plane by spacecraft close to Earth's orbit, the fast solar wind with speeds averaging 700 km s^{-1} was associated with polar coronal holes with an equatorward extension (Krieger, Timothy, & Roelof 1973) or with the faster than radial divergence of their boundaries reaching low latitudes with the tilt of the axis of the solar dipole (see Hundhausen 1977). In fact, the predominance of the fast solar wind over a large fraction of the heliosphere, from polar measurements by *Ulysses* during a significant portion of the solar cycle away from maximum, has been attributed to the rapid divergence of coronal hole boundaries identified with adjacent streamers (Gosling et al. 1995). Recent quantitative analyses of the latitudinal variations of the polarized brightness emission (pB) combined with radio occultation (Woo & Habbal 1997) and in situ measurements (Habbal & Woo 2001), however, have led to a different conclusion. These

authors showed that the fast solar wind did not originate solely from coronal holes, but rather expanded mostly radially from a significant fraction of the so-called quiet Sun (i.e., the solar surface away from active regions). These results thus pointed to the existence of open magnetic flux (i.e., flux that extends from the Sun into interplanetary space) from a large fraction of the solar surface.

Resonance scattering, which contributes to the formation of a number of coronal forbidden lines, had been recognized several decades ago as a tool for studying the direction of the coronal magnetic field (e.g., Charvin 1965; House 1974; Arnaud 1983). The polarization of these lines is produced only by resonance scattering. Given the estimated strength of the magnetic field in the corona, the direction of polarization is expected to be either parallel or perpendicular to the field direction projected onto the plane of the sky (Charvin 1965; House 1974). Early investigations utilizing this technique during total solar eclipses with observations of the Fe XIII 10747 Å (Eddy, Lee, & Emmerson 1973) and Fe XIV 5303 Å lines (Picat et al. 1979) proved its feasibility. However, it was not until a dedicated observing program was underway at the observatories of Pic du Midi (initiated by P. Charvin and realized by J. Arnaud) and Sacramento Peak (initiated by G. Newkirk and realized by the High Altitude Observatory [HAO] under the leadership of C. W. Querfeld) that the power of this technique was satisfactorily proven (see Arnaud 1982a, 1982b, 1983; Arnaud & Newkirk 1987). That the direction of the coronal magnetic field was predominantly radial, independent of the phase of the solar cycle, was the striking result to emerge consistently from all these observations.

In this paper, the polarized intensity measurements of the Fe XIII 10747 Å line described by Arnaud (1983) are placed, for the first time, in the context of the corresponding pB

images from the HAO Mauna Loa MkIII K-Coronameter, which first became available in 1980. It is shown how the predominance of the radial direction of the coronal magnetic field at solar maximum is consistent with radially expanding magnetic field lines coexisting with the large-scale structures associated with streamers.

2. POLARIZATION OF THE Fe XIII 10747 Å LINE: THEORETICAL CONSIDERATIONS AND OBSERVATIONS

The theory of coronal emission-line polarization has been extensively developed over the past three to four decades (e.g., Charvin 1965; Hyder 1965; Sahal-Bréchet 1974; House 1972, 1977; and more recently Casini & Judge 1999). The preferred alignment of the magnetic dipole moments of ions along the coronal magnetic field leads to polarized emission through the process of resonance scattering (also known as resonance fluorescence) of the anisotropic distribution of the unpolarized photospheric light. The Fe XIII 10747 Å and Fe XIV 5303 Å emission lines in the near-infrared and visible are the most suitable coronal lines for polarization measurements.

In regions of the corona where the density is high, these spectral lines are formed preferentially by collisional excitation, hence no polarized emission will be measured. For lower density regions, in particular further out in the corona where the density decreases with radial distance, resonance scattering dominates, the polarization rate increases, and the intensity decreases. In addition to depolarization due to collisional excitation, magnetic inhomogeneities along the line of sight and propagation of the incident solar disk radiation at large angles with respect to the coronal magnetic field direction, contribute to the depolarization of the lines. For angles larger than the Van Vleck angle of 54.7° , the direction of polarization becomes perpendicular to the magnetic field, and the polarization is reduced compared to its value before this "flipping." Model calculations of the coronal emission line polarization of Fe XIII 10747 Å by House (1977) showed that the maximum polarization was significantly lower in the case of a dipole field compared to a radial field.

Several attempts at coronal line polarimetric measurements were made as early as 1900 (Wood 1906). However, it was not until 1977 that a comprehensive observing program was underway at Pic du Midi for the Fe XIV 5303 Å polarization measurements. Concurrently, a coronal emission-line polarimeter (KELP) was operated by HAO in collaboration with the Sacramento Peak Observatory for the polarization measurement of Fe XIII 10747 Å (see Arnaud 1983). The program ended in 1980. The latter measurements covered heights between 1.1 and $2 R_\odot$, with a spatial resolution of $1'-2'$ depending on sky conditions and height in the corona. Each height was scanned in 128 sequential measurements equally spaced in position angle.

Comparison of the Fe XIII and Fe XIV studies (Arnaud 1984) showed that the polarization of Fe XIII was 11.6% on average compared to a much weaker polarization of 1.6% for Fe XIV. While contributions along the line of sight will reduce the percent polarization, they will not change the direction of polarization of what lies in the plane of the sky. Hence, the observed predominance of a radial field implies that this is the dominant field direction in the plane perpendicular to the line of sight.

3. COMPARISON OF POLARIZATION MAPS AND POLARIZED BRIGHTNESS IMAGES

Because the Fe XIII line is stronger than the Fe XIV line, has a higher degree of polarization, can be detected out to at least $2 R_\odot$ in the corona, and has a broader temperature coverage, it is the more desirable spectral line to pursue in the comparison of polarized intensity maps with pB images. The present study is limited to the observations of 1980 when pB images of the solar corona first became available, on the last year of the KELP observing program.

Observations from 1980 February 23 (day of year [DOY] 54) and April 1 (DOY 92) are shown in Figures 1 and 2, respectively, and two north-east-south hemispheres from September 1 (DOY 245) and 2 (DOY 246) in Figure 3. These were selected from dates when the best spectral line polarization measurements were obtained as a result of ideal weather conditions and when pB images from the HAO Mauna Loa MkIII K-Coronameter were available. We concentrate first on Figures 1 and 2. To illustrate the differences, as well as correspondences, between these measurements, the Fe XIII polarized intensity map (*left panel*), the pB image (*right panel*), and their superposition (*lower panel*) are given sequentially in these figures. In the polarization maps, the length of the line segments is proportional to the polarized intensity, pI , i.e., the percent polarization, p , multiplied by the intensity of emission, I , at that given position in the plane of the sky. The orientation of the segments gives the direction of polarization. Observations were made at $1.1 R_\odot$, $1.2-1.55 R_\odot$ in increments of $0.05 R_\odot$, and at 1.64 , 1.7 , and $1.8 R_\odot$ for DOY 54. For DOY 92, they cover 1.15 to $1.55 R_\odot$, also in increments of $0.05 R_\odot$. For ease of reference, the tick marks on the left panels give the position angle, P.A., every 10° . P.A. is measured counterclockwise starting from 0° north.

In general, the polarized intensity maps reflect a predominant radial field. There are, on average, two different levels of pI , with values above 60° latitude being half their values below 60° , as reported originally by Arnaud (1983). All values become more uniform beyond $1.25 R_\odot$. The pB images, on the other hand, are typical of a corona at solar maximum, dominated by streamers at all latitudes, as would be the case for 1980. The comparison between pI and pB becomes more striking with the superposition of the pI map and pB image. Several expected, as well as unexpected, results emerge.

We consider first the regions of reduced or absent polarized emission. One occurs in the south polar region around P.A. = 180° , which has a larger angular extent on DOY 92 than on DOY 54. In the corresponding pB images, this area is characteristic of a polar coronal hole. Indeed, a lower density and temperature can readily account for the absence of Fe XIII emission. Surprisingly, however, the region at P.A. = 320° on DOY 54, which has the same pB value at $1.15 R_\odot$ as in a coronal hole at solar minimum, has polarized emission starting at $1.2 R_\odot$, as seen within the wedge (A) in Figure 1. The same is found in Figure 3 for September 1 and 2 at P.A. = $0^\circ-20^\circ$.

The absence of pI can also result from depolarization effects due to the dominance of collisional excitation compared to radiative emission in high density regions. This is evident close to the solar limb where pB is enhanced, such as on DOY 92 (Fig. 2) at $1.15 R_\odot$ for P.A. = 35° , 55° , $70^\circ-100^\circ$, $120^\circ-140^\circ$, $220^\circ-280^\circ$, and $300^\circ-340^\circ$. For P.A. = 70°

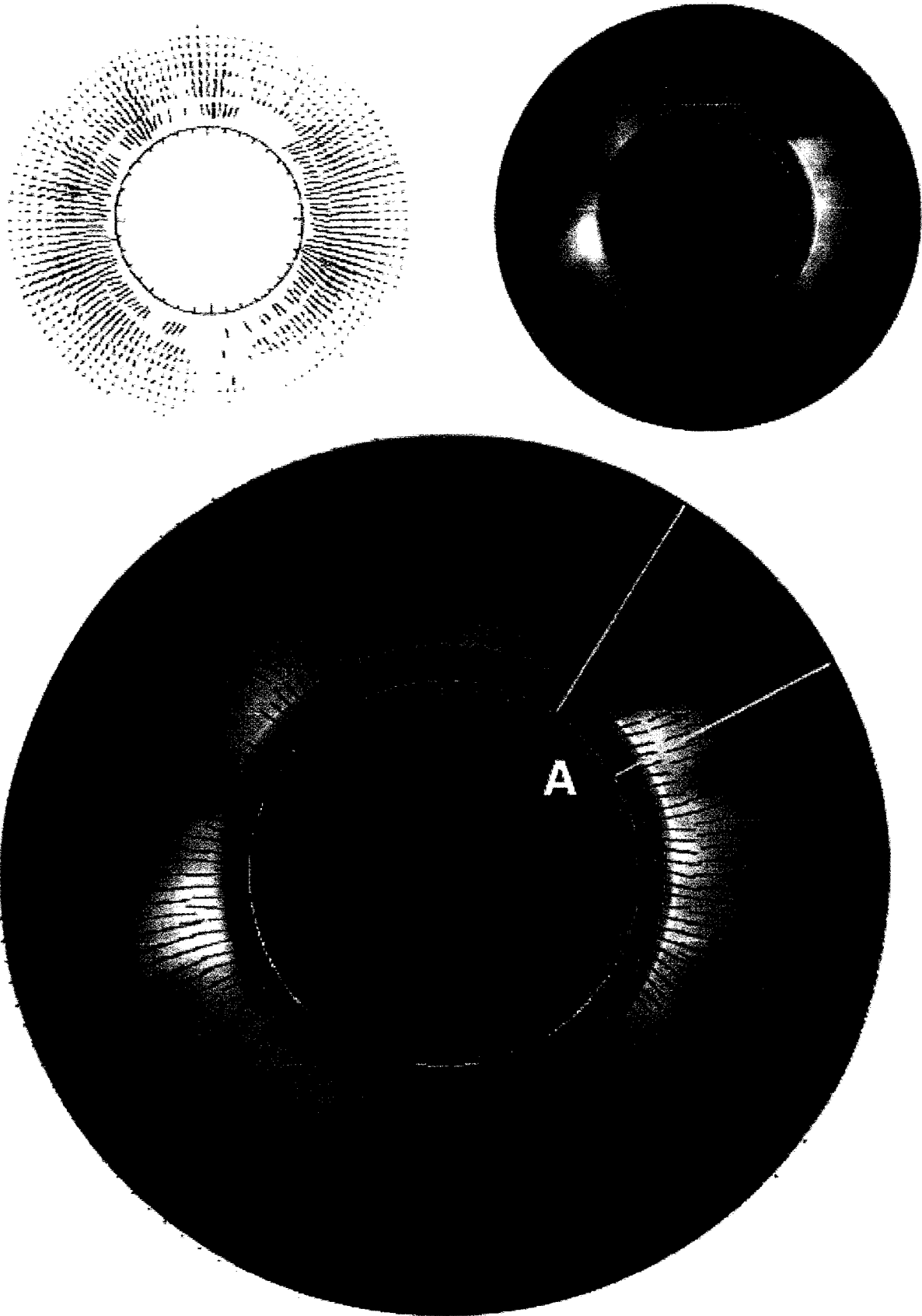


FIG. 1.—Polarized intensity maps of the Fe XIII Å line emission taken from Sacramento Peak (*left*), *pB* image from the Mauna Loa K-Coronameter (*right*), and an overlay of the two (*lower panel*), for observations made on 1980 February 23 (DOY 54). The orientation of the segments gives the direction of polarization, while their lengths are proportional to pl . Tick marks on the left and lower panels at the position of the occulted Sun, give position angle, P.A., in increments of 10° . The wedge (A), within the two yellow lines, isolates a streamer and its vicinity, illustrating in this case how there is no marked difference in polarization direction between the region coinciding with the streamer seen in white light and that directly adjacent to it.

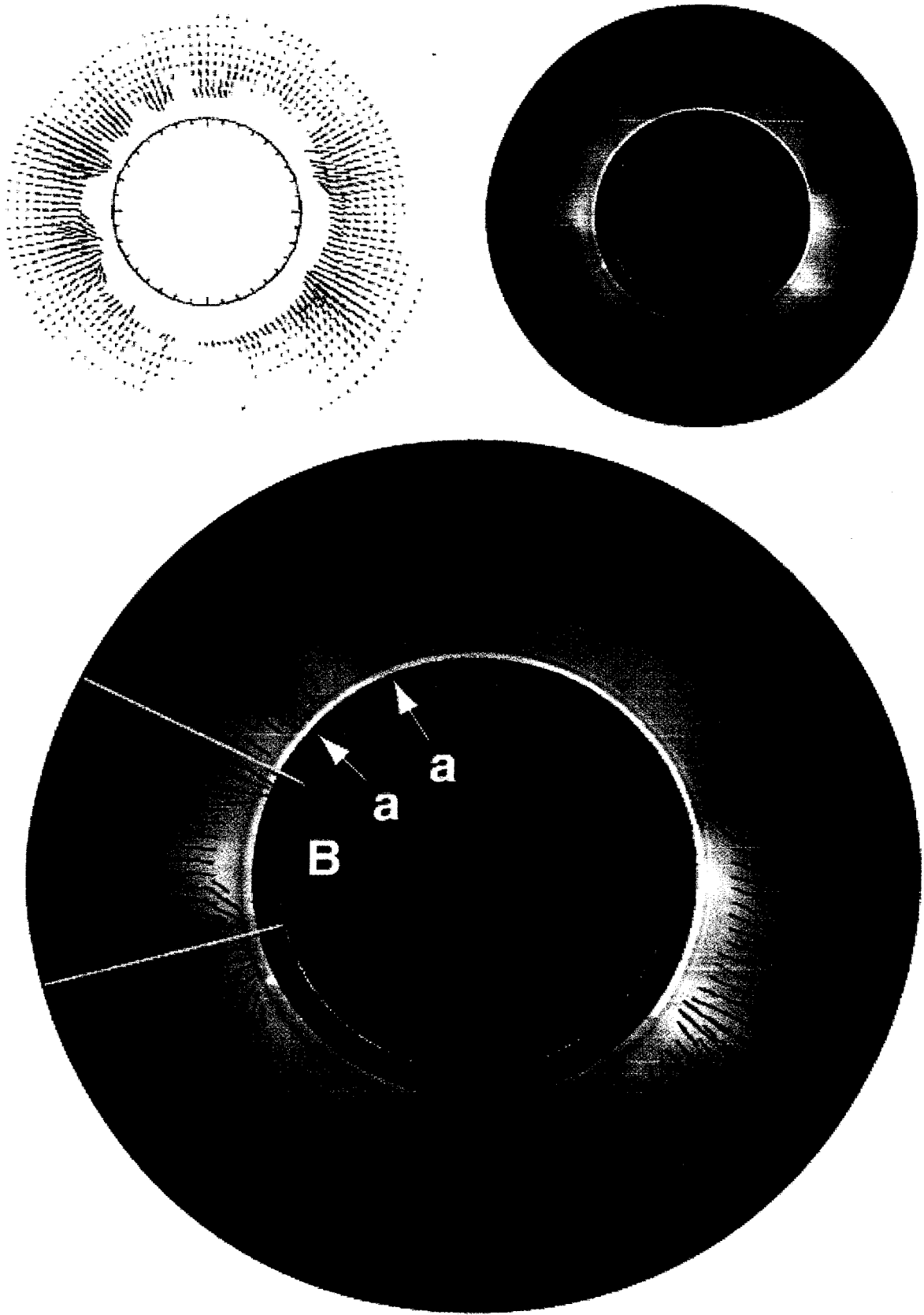


FIG. 2.— Same as Fig. 1 for 1980 April 1 (DOY 92). Arrows (a) point to regions of enhanced pI between streamers. The wedge (B) isolates a streamer and its vicinity where the effects of depolarization close to the Van Vleck angle are evident at the base of the streamer.

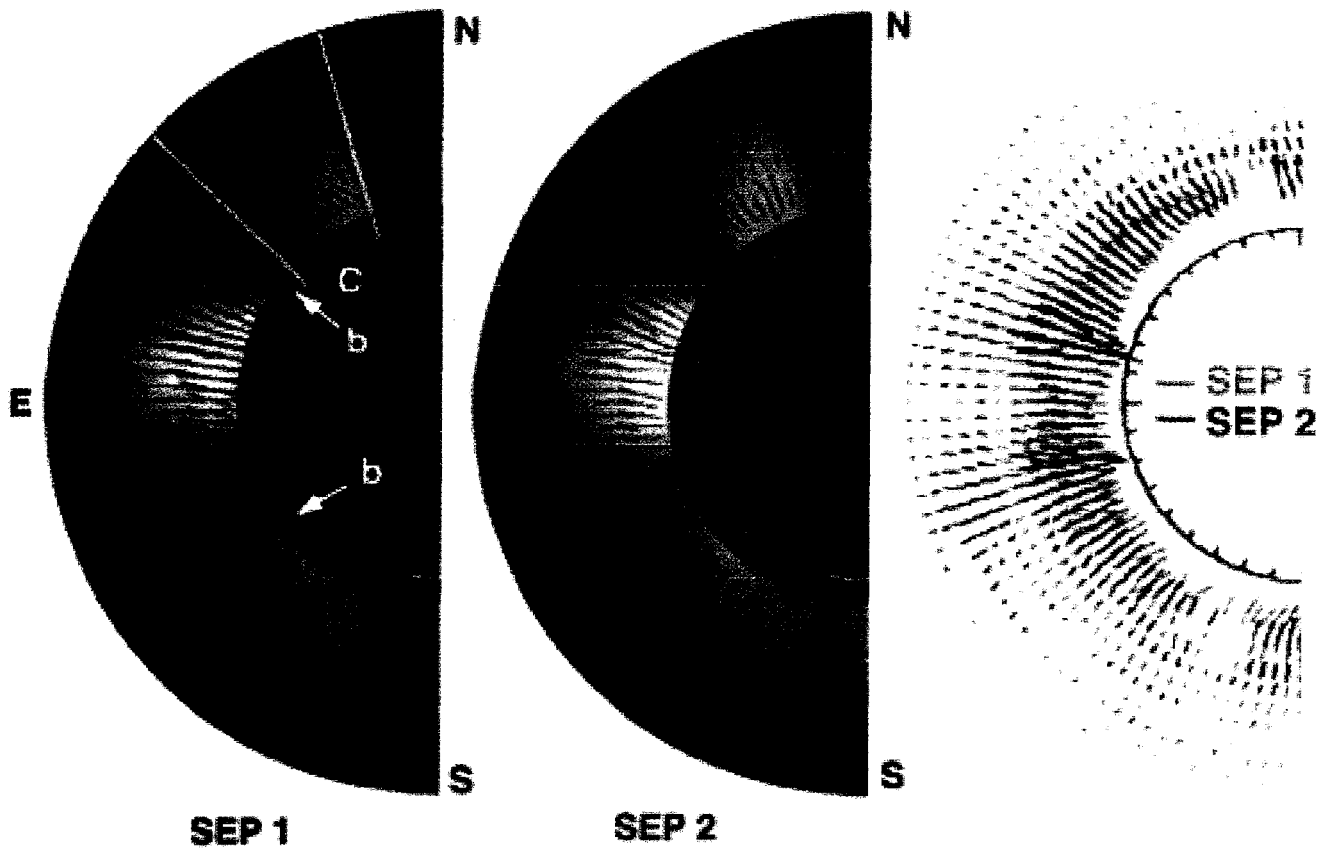


FIG. 3.—North-east-south hemispheres of an overlay of pI maps and pB images for 1980 September 1 (DOY 245) and 2 (DOY 246). The overlay in the right panel of the pI maps only (for DOY 245 [blue] and DOY 246 [red]) shows that the polarization direction associated with the streamers changes with rotation, while the radial direction is pervasive and does not change on the two consecutive days. The wedge (C) isolates a streamer and its vicinity where the direction of polarization at the base of the streamer seems to be in the opposite direction from that inferred from white light. A radial alignment in the polarization direction is observed thereafter throughout the wedge. Arrows (b), like those (a) in Fig. 2, point to regions of enhanced pI between streamers.

100°, the depolarization is most likely due to the propagation at the Van Vleck angle of 54°7, as evidenced by the direction of polarization being close to 50° on either side of the base of the streamer between P.A. = 80° and 100°. In this case, as the angle between the radial direction of the incident radiation from the disk and the magnetic field direction increases beyond 50° toward the center of the streamer, the polarized emission disappears. Other possible cases of depolarization at the Van Vleck angle are at P.A. = 120° and 290° on DOY 92. These instances are very likely to occur in the presence of looplike structures in the plane of the sky at the base of streamers. It is however surprising to find that no such depolarization is observed on DOY 54 (Fig. 1) even though pB is also enhanced close to the limb. A complex magnetic pattern along the line of sight which cannot be inferred from pB images can also lead to depolarization. This could account for the instances when depolarization is observed without enhanced pB , such as on DOY 54, P.A. = 310°–340° below 1.2 R_{\odot} (Fig. 1), and on DOY 245 and 246 for P.A. = 20°–70° (Fig. 3).

Enhanced pI -values characterized by longer radial segments, which appear everywhere at the boundaries between streamers, are a feature common to all days. These are indicated by arrows labeled “a” in Figure 2, and labeled “b” in Figure 3. For DOY 54 (Fig. 1) they are at P.A. = 0°, 30°–40°, 60°–120°, and 240°–310°. For DOY 92 (Fig. 2), they appear at 1.2 R_{\odot} (since, as described earlier, pI is predominantly absent very close to the Sun in this example) and are observed at P.A. = 0°, 25°–70°, 90°–120°, 220°–250°, and

280°–300°. On the other hand, while the predominant direction of polarization is radial, there are several instances where the polarization direction drifts from the radial direction, in particular close to the limb. These are most evident in the example of Figure 2 at P.A. = 60°–70°, 90°–100°, 120°, and 290°–310° and in Figure 3, on September 1, for P.A. = 20°–50° and 90°–120°. A few instances of departure from radial are found at larger heliocentric distances, such as in Figure 1 at P.A. = 70°, 80°, and 120°.

The most unexpected and surprising result to emerge from the comparison of pI and pB , however, is the fact that the direction of polarization does not always match the underlying direction of the streamers as seen in white light. Examples comparing different associations between pI and pB in streamers and their vicinity are shown within the wedges labeled “A,” “B,” and “C” in Figures 1, 2, and 3, respectively. The most striking example is that of DOY 54 (Fig. 1) at P.A. = 40°–60°, 80°–110°, and 300°–320° when streamers seem to curve around as they taper off. In the wedge (A), for example, with the exception of the first row of polarization segments at the base of the streamer, there is no marked difference in polarization direction between the region coinciding with the streamer seen in white light and that directly adjacent to it, even though the streamer in white light seems to follow a different direction. This was also noted by Eddy et al. (1973), with the more limited field of view of their eclipse observations, and at a different phase of the solar cycle. In example B on DOY 92 (Fig. 2), the streamer appears to be radially aligned and symmetrical in

the plane of the sky, and there is no difference in the direction of polarization along the streamer and within its vicinity. In C (Fig. 3), the polarization direction at the base of the streamer seems to be exactly opposite to that of the direction in the pB image, and the radial alignment of the polarization direction along the streamer and its vicinity occurs at larger heliocentric distances than in the other two examples.

To explore how the presence of a streamer in the plane of the sky only affects the direction of polarization associated with it, we make use of solar rotation with observations on two consecutive days. The change in polarization direction from one day to the next in the inner corona below $1.75 R_{\odot}$ can be seen in the third panel of Figure 3 from the superposition of the two polarization maps. The largest changes occur at P.A. = 20° – 40° and 80° – 120° , which coincide with the base of two streamers. In the rest of the corona the polarization direction does not change as would be expected for a predominant radial field. The change in polarization direction as a function of rotation shows how the magnetic field direction in the plane of the sky changes from one day to the next, a fact that is not evident in the pB images. To further quantify the differences in pB observed on these consecutive days, the corresponding latitudinal profiles measured at $1.15 R_{\odot}$ and $1.74 R_{\odot}$ versus P.A. from 0° to 180° are plotted in Figure 4. When the streamer rotates into the plane of the sky, pB should increase. This is indeed observed for the streamers centered at 80° and 104° ,

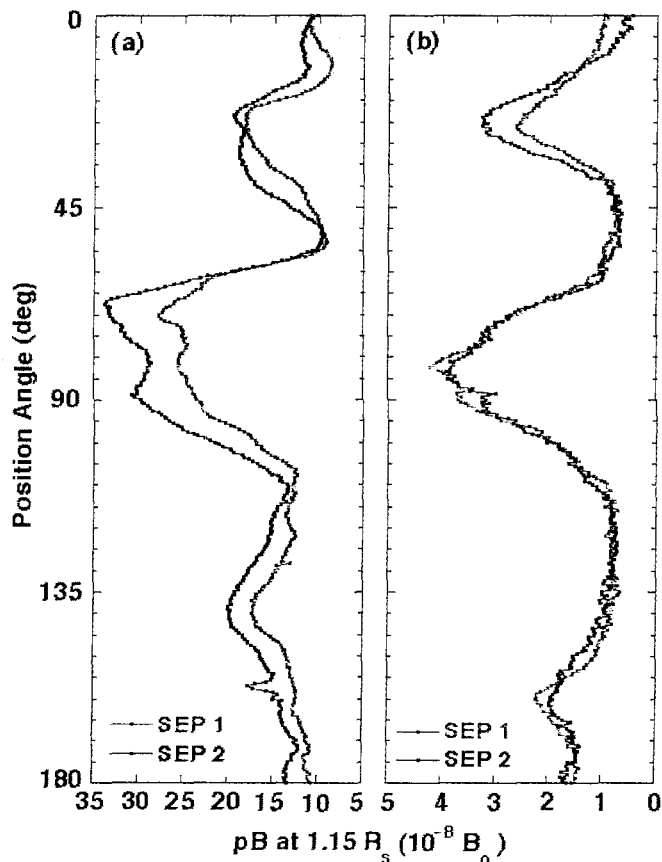


FIG. 4.— Latitudinal profiles of pB (horizontal axis) vs. P.A. (vertical axis) measured at (a) $1.15 R_{\odot}$ and (b) $1.74 R_{\odot}$. The orientation of the plots was chosen to make the comparison with the hemispheres in Fig. 3 for DOYs 245 (red) and 246 (blue) more straightforward.

since the pB value at $1.15 R_{\odot}$ is higher on DOY 246 (blue line) than on DOY 245 (red line). This is also where the polarization direction changed the most. The pB measurements at $1.74 R_{\odot}$ do not show any significant variation between the two days, indicating that the radial field dominates all latitudes at that height.

4. DISCUSSION AND CONCLUSIONS

The comparison of pI and pB images from 1980 makes it rather straightforward to account for the observed depolarization due to the predominance of collisional excitation, propagation at the Van Vleck angle, and low density regions. More importantly, this comparison makes it evident that using pB images alone is not a reliable approach for the inference of the direction of the coronal magnetic field in the plane of the sky.

The most striking result to emerge from the comparison of pI maps and pB images, however, is that there seems to exist two components to the coronal magnetic field. One component is associated with the large-scale structure of streamers with looplike structures at their base. The other more prevalent component is the predominantly radial one which corresponds to the “open” coronal magnetic field. The latter seems to infiltrate most coronal density structures as it is observed in the plane of the sky even where the streamers evolve in shape with distance, as shown in the comparison of the direction of polarization overlaying a streamer and its vicinity. This is also most strongly demonstrated when a streamer moves in and out of the plane of the sky. The findings presented here thus yield further supporting evidence for the observed prevalent radial expansion of coronal density structure from a significant fraction of the solar surface (Woo & Habbal 1999) and their filamentary nature (Woo 1996).

The comparison of polarized line emission with polarized brightness provides the heretofore missing connection between the photospheric field and its extension into the corona. In particular, it suggests that the strong- and weak-field components of the quiet-Sun photospheric field, recently observed by Lin (1995) and Lin & Rimmele (1999), and supported by theoretical investigations of the solar dynamo (e.g., Cattaneo 1999), have a counterpart in the corona where they coexist. The absence of solar cycle dependence in the predominance of the radial direction of the coronal magnetic field, derived from observations at different stages of the solar cycle by Eddy et al. (1973) and Arnaud (1983), and the negligible solar cycle dependence of the distribution of the photospheric flux below 25 G (Harvey 1994) suggest that it is again the weak-field component that defines the open magnetic field in the quiet corona.

At present, polarimetric measurements are the only tool to yield the direction and distribution of the open flux in the corona. The predominance of a radial magnetic field direction throughout the corona, threading even the regions containing streamers, has not shown up in any modeling so far, most likely because the weaker photospheric field component is neglected in the extrapolation process. Interestingly, it is this component which seems to dominate the distribution of open magnetic flux in the corona.

The first Zeeman effect measurements in the corona using the circular polarization of the 10747 \AA line, recently made by Lin, Penn, & Tomczyk (2000), yield the magnetic field

strength along the line of sight with no information, however, about the field direction. The linear polarization, on the other hand, provides the field direction in the plane of the sky but is not sensitive to the field strength. Hence, linear and circular polarization measurements should be considered complementary and are critical in future investigations of the coronal magnetic field.

Despite the recent success of the *SOHO* and *TRACE* missions, measurements of one of the most critical physical parameters, namely the coronal magnetic field, were missing. The results of this study show how, by synthesizing polarimetric observations of spectral lines and white light, one arrives at a different view of the expansion of the solar magnetic field in the corona than what emerges from white light (and extreme ultraviolet) images alone. Although it is not a straightforward task to reconstruct the coronal magnetic field from polarimetric measurements alone, the diagnostic tool provided by daily polarimetric observations with high spatial resolution should be seriously considered as an integral element of future solar missions if we are to

explore and understand the coronal magnetic field. Another interesting by-product of such observations would be the inference of the longitudinal extent of coronal streamers as they rotate in and out of the plane of the sky. The elimination of the contribution of the large-scale streamer structures, which changes with solar rotation, should then yield the distribution of the dominant component of the coronal magnetic field that extends into interplanetary space and carries the solar wind.

This work was done while S. R. Habbal was Chercheur Associé of the CNRS at IAS in Orsay. R W.'s research was supported by a contract with NASA to the Jet Propulsion Laboratory, California Institute of Technology. The KERP measurements would not have been made possible without the joint efforts of HAO and Sacramento Peak Observatory. The *pB* data are from the MkIII K-Coronameter which is operated by NCAR/HAO. We thank C. Copeland for her technical help with the preparation of the figures.

REFERENCES

- Altschuler, M. D., & Newkirk, G. A., Jr. 1969, *Sol. Phys.*, 9, 131
 Arnaud, J. 1982a, *A&AS*, 112, 350
 ———. 1982b, *A&AS*, 116, 248
 ———. 1983, Ph.D. thesis, Univ. Paris VI
 ———. 1984, in *Proc. 4th European Meeting on Solar Physics (ESA SP-220)*, 115
 Arnaud, J., & Newkirk, G., Jr. 1987, *A&AS*, 178, 263
 Casini, R., & Judge, P. G. 1999, *ApJ*, 522, 524
 Cattaneo, F. 1999, *ApJ*, 515, L39
 Charvin, P. 1965, *Ann. d'Astrophys.*, 28, 877
 Eddy, J. A., Lee, R. H., & Emerson, J. D. 1973, *Sol. Phys.*, 30, 351
 Gosling, J. T., et al. 1995, *Geophys. Res. Lett.*, 22, 3329
 Habbal, S. R., & Woo, R. 2001, *ApJ*, 549, L253
 Harvey, K. L. 1994, in *IAU Colloq. 143, The Sun as a Variable Star: Solar and Stellar Irradiance Variations*, ed. J. Pap, C. Frölich, H. Hudson, & S. Solanki (Cambridge: Cambridge Univ. Press), 217
 House, L. L. 1972, *Sol. Phys.*, 23, 103
 House, L. L. 1974, *PASP*, 86, 490
 ———. 1977, *ApJ*, 214, 632
 Hundhausen, A. 1977, in *Skylab Workshop on Coronal Holes and High Speed Streams*, ed. J. Zirker (Boulder: Colorado Univ. Press), 225
 Hyder, C. L. 1965, *ApJ*, 141, 1382
 Krieger, A. S., Timothy, A. F., & Roelof, E. C. 1973, *Sol. Phys.*, 23, 123
 Lin, H. 1995, *ApJ*, 514, 421
 Lin, H., Penn, M. J., & Tomczyk, S. 2000, *ApJ*, 541, L83
 Lin, H., & Rimmele, T. 1999, *ApJ*, 514, 448
 Linker, J. A., et al. 1999, *J. Geophys. Res.*, 104, 9809
 Picat, J. P., Felenbok, P., Fort, B., & Groupe Caméra Electronique. 1979, *A&AS*, 75, 176
 Sahal-Bréchet, S. 1974, *A&A*, 32, 147
 Woo, R. 1996, *Nature*, 379, 321
 Woo, R., & Habbal, S. R. 1997, *Geophys. Res. Lett.*, 24, 1159
 ———. 1999, *Geophys. Res. Lett.*, 26, 1793
 Wood, R. W. 1906, *Publ. US Naval Obs.*, 4, D112